Tu B1 10

The Benefits of Simultaneous Shooting on Land for Improved Productivity and Enhanced Data Quality through Dense Source Sampling

D. McCarthy* (CGG), A. Berhaud (CGG), S. Mahrooqi (PDO), G. Henin (CGG), J. Shorter (PDO)

Summary

Difficulties in processing land seismic data often arise due to insufficient sampling of the wavefield, resulting in poor near surface imaging, and aliasing of coherent noise forms such as surface waves. These problems can be mitigated by improving the wavefield sampling through denser acquisition. Fully unconstrained simultaneous shooting offers a way to substantially increase productivity and hence source densities. However, in order to achieve this we must be able to separate the signal from the interference noise generated by the blended acquisition. Using a de-blending routine based on inverse problems in the curvelet domain (Guillouet et al., 2016) the following case study from The Sultanate of Oman demonstrates the benefits of dense source sampling for broadband, wide-azimuth land data acquired using simultaneous shooting.

Introduction

Blended acquisition, or simultaneous shooting, is a very attractive scheme for land acquisition as it enables high vibroseis productivity and the possibility of high sampling in the source domain. To fully benefit from the productivity enhancements of blended data it is necessary to be able to separate the signal from the interference or cross-talk noise, a step commonly referred to as de-blending. In the following case study we will show an example where dense, wide-azimuth (WAZ), broadband land data have been acquired using unconstrained, blended, simultaneous shooting and successfully de-blended using a curvelet domain inversion scheme (Guillouet et al., 2016). The results from the de-blending are compared with a sparser base production dataset acquired using slip-sweep distance separated simultaneous source (DS^3) acquisition (Bouska, 2010). In addition to the successful de-blending of the data, the case study will highlight advantages of high sampling in the source domain, which include; improved ground roll imaging and attenuation; improved imaging of the near surface on pre-stack time migrated sections (PreSTM); and improved pre-stack amplitude variation with offset and azimuth (AVO/AVOA) attributes.

Acquisition

The blended data were acquired as a separate test during the acquisition of a large 3D, broadband, WAZ survey in Oman using slip-sweep DS^3 shooting acquisition (Bouska, 2010) (which will be referred to as the base production data for the rest of this paper). A total of 12 vibrators were used for the blended acquisition test and shots were acquired on a dense 12.5 m × 12.5 m grid within a 2 km × 10 km polygon overlying the on-going base production data. Each vibrator was assigned to an individual sector within the shot polygon of dimensions 1 km × 2 km and a condition was imposed that a minimum separation of 1 km was to be maintained between adjacent vibrators at all times. The vibrators were otherwise completely autonomous, using the same 9 s sweep from 1.5 Hz to 76 Hz and were on local mode, vibrating when on point. The data were recorded on a fixed, continuously recording receiver spread of dimensions 1.4 km by 10 km, consisting of 14 cables separated by 100 m, with a receiver spacing of 25 m. This was the exact same receiver spread used to record the base production data, which were acquired with a 50 m × 50 m source grid. During the test approximately 120,000 shots were recorded over 5 days of shooting, averaging 24,000 vibrator points (VPs) per day. The resulting blended dataset had a trace density of 128 million traces/km^2, 16 times denser than the base production data at 8 million traces/km^2. The 12.5 m × 12.5 m dataset was decimated during processing in order to simulate acquisition on a 25 m × 25 m shot grid.

Processing Sequence

The acquired data were de-blended based on the recovery of sparse signal in the 3D curvelet domain by solving an inverse problem (Guillouet et al.,2016). Figure 1 shows the result of the de-blending routine on a raw shot gather, (a) is the blended shot gather, (b) the de-blended result and (c) the difference between (a) and (b). It is clear from this example that the signal has been successfully separated from the cross-talk noise with no apparent leakage. Figure 2 compares a shot from the blended acquisition with a shot from the base production data at the same surface location, (a) is the blended shot gather, (b) the de-blended result and (c) the base production shot gather. The resulting de-blended shot gather is very similar to the base production acquisition shot gather in terms of the signal character. Once de-blended, the data were decimated to a 25 m × 25 m grid and both the original 12.5 m × 12.5 m and the decimated data were processed to PreSTM using an advanced processing sequence designed for dense, WAZ, broadband land datasets. The production acquisition data were used as a baseline to compare with the de-blended and decimated de-blended data, with shots extracted from the same source polygon of 2 km × 10 km, going into the same 14 receiver lines to enable a fair comparison between all three datasets.

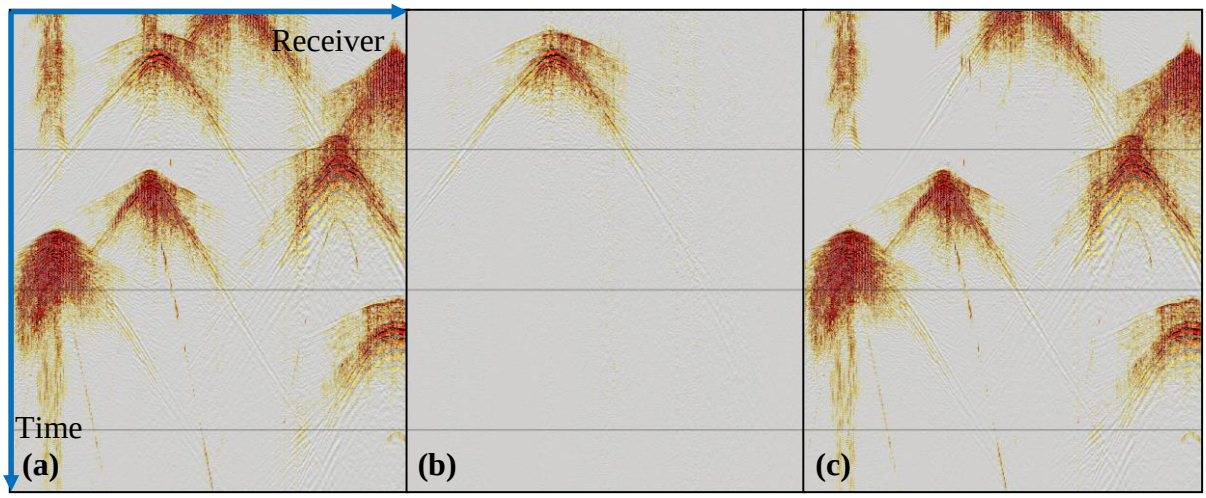

Figure 1 *Raw shot gather, (a) before de-blending, (b) after de-blending and (c) the difference between (a) and (b). From this example it is clear that the de-blending routine can remove the interference noise without signal leakage.*

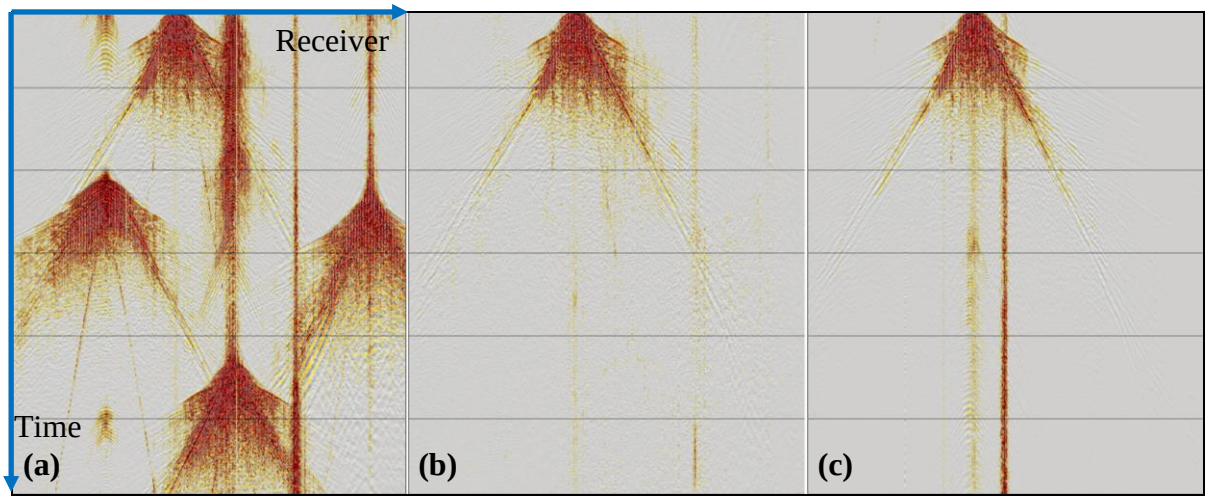

Figure 2 *Raw shot gather, (a) before de-blending, (b) after de-blending and (c) raw shot gather from the base production data at the same location. The resulting de-blended shot gather closely resembles the base production gather in terms of signal character.*

Figure 3 shows both the base production data and the 12.5 m × 12.5 m de-blended data at the ground roll attenuation stage of the processing, (a) shows a cross-spread from the base production data with a 50 m source spacing and its associated FK spectrum, there is clear aliasing of the ground roll from approximately 12 Hz, (b) shows the same cross-spread after adaptive ground roll attenuation (Le Meur et al. 2008), although the ground roll attenuation has done a good job there is still residual aliased noise remaining, (c) shows a common receiver gather (CRG) with a 12.5 m source spacing at the same location from the de-blended dataset, the imaging of the ground roll is improved due to the dense source sampling, (d) the CRG from (c) after adaptive ground roll attenuation, compared with (b) the CRG is much cleaner with all of the ground roll attenuated and no aliased noise remaining. This example highlights one advantage of dense source sampling, which is made possible through unconstrained simultaneous vibroseis recording due to the increase in productivity. The improved sampling of the ground roll will also improve surface wave dispersion curve picking, which can be used for joint inversion using surface waves and refracted p-waves for building an accurate near surface velocity model (Duret et al., 2016).

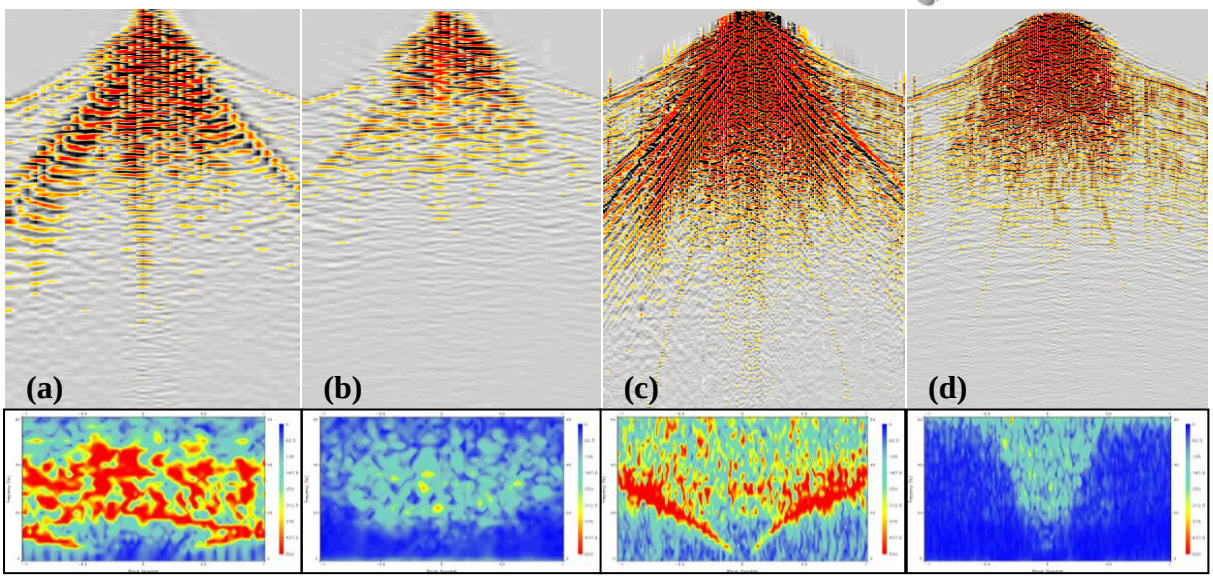

Figure 3 *Cross-spreads before and after ground roll attenuation, with their associated FK spectra (a) base production data cross-spread with 50 m spacing between shots before ground roll attenuation, (b) the same cross-spread after ground roll attenuation, (c) a common receiver gather (CRG) from the de-blended dataset with 12.5 m spacing between shots, (d) the same CRG after ground roll attenuation. This example clearly illustrates the advantages of dense sampling for accurate ground roll imaging and attenuation.*

Results

Figure 4 shows a comparison between the final PreSTM sections for (a) the base production dataset, (b) the de-blended dataset and (c) the decimated de-blended dataset. There is a clear improvement in the imaging of near surface events (as highlighted by blue arrows) on the de-blended data, as a direct result of the denser source sampling. The example shows that the denser the shot grid, the better the result, (b) is 16 times denser than (a) and has a greater improvement in the near surface compared to (c), which is only 4 times as dense. It is also important to examine the quality of the pre-stack data and Figure 5 shows the results of AVO/AVOA analysis carried out over a shallow horizon from the base production and de-blended datasets, (a) shows the intercept for the base production, de-blended and decimated de-blended data respectively, (b) shows the gradient, (c) the anisotropic gradient and (d) the Phi angle. As for the PreSTM section, trace density plays an important role in the AVO/AVO attributes with the cleanest, sharpest results coming from the de-blended data (16 times denser than the base production), then the decimated de-blended data (4 times denser) and finally the base production data.

Conclusions

This case study has demonstrated the ability to acquire blended seismic data sets with increased productivity and to successfully separate signal from interference noise, using a 3D curvelet domain based inversion, on data acquired using simultaneous shooting. Raw shot gathers before and after de-blending show the removal of interference and harmonic noise with no signal leakage. Acquiring data using simultaneous shooting opens the way to increase source sampling while maintaining high productivity. The results from this case study demonstrate some of the advantages of dense source sampling, which include; improved ground roll imaging and attenuation; improved near surface imaging; and superior AVO/AVOA results.

Acknowledgements

We are grateful to the Ministry of Oil and Gas of the Sultanate of Oman and Petroleum Development of Oman for permission to present the data examples.

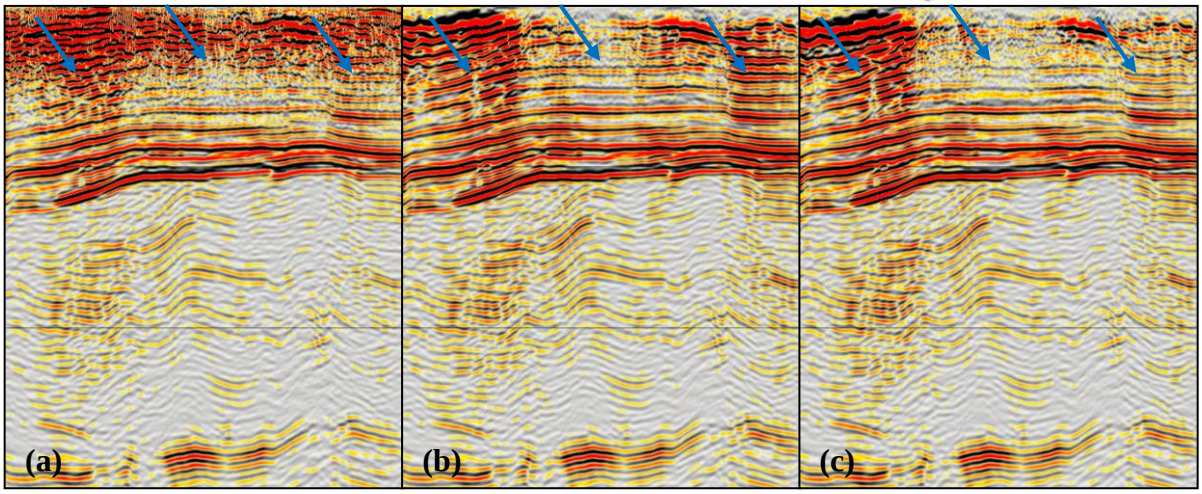

Figure 4 *Final PreSTM section for (a) base production data, (b) de-blended data and (c) decimated de-blended data. The blue arrows highlight shallow reflectivity, which is imaged more clearly in both the de-blended and decimated de-blended data as a result of higher trace density.*

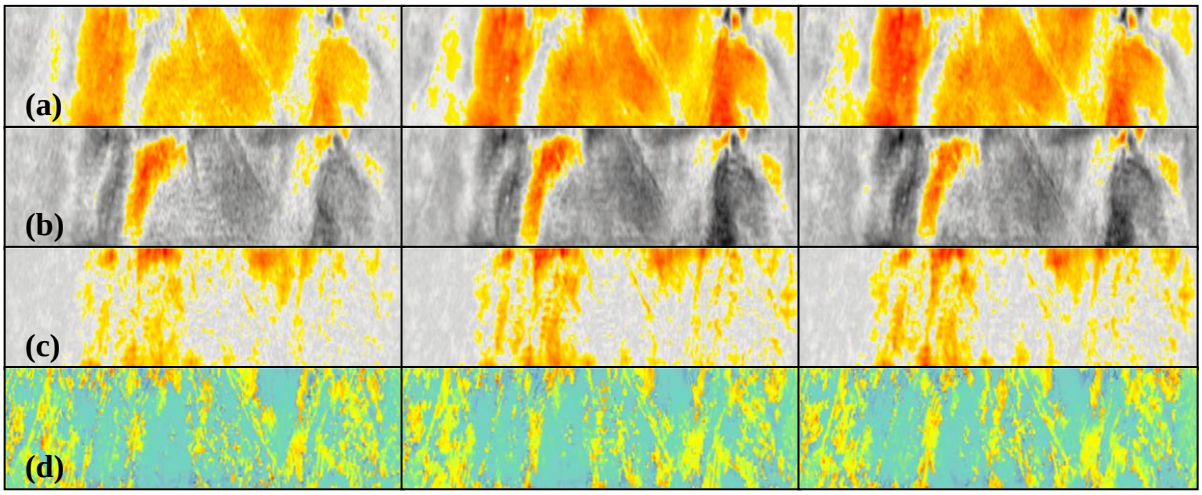

Figure 5 *From left to right shows the AVO/AVOA attributes from the base production, de-blended and decimated de-blended datasets, (a) intercept, (b) the gradient, (c) the anisotropic gradient and (d) the phi angle. A general improvement in all the attributes is seen in the de-blended and decimated de-blended data as a result of the higher trace density.*

References

Bouska, J. [2010] Distance separated simultaneous sweeping, for fast, clean, vibroseis acquisition. *Geophysical Prospecting*, **58**, 123-153.

Duret, F., Bertin, F., Garceran, K., Sternfels, R., Bardainne, T., Deladerriere, N. and Le Meur, D. [2016] Near-surface velocity modeling using a combined inversion of surface and refracted P-waves. *The Leading Edge*, 35(11):936-941.

Guillouet, M., Berthaud, A., Bianchi, T. and Pignot, G. [2016] Recovery of blended data: a sparse coding approach for seismic acquisition. *78th Conference & Exhibition, EAGE,* Extended Abstracts.

Le Meur, D., Benjamin, N., Cole, R. and Harthy, M. [2008] Adaptive Groundroll Filtering. *70th Conference & Exhibition, EAGE,* Extended Abstracts.